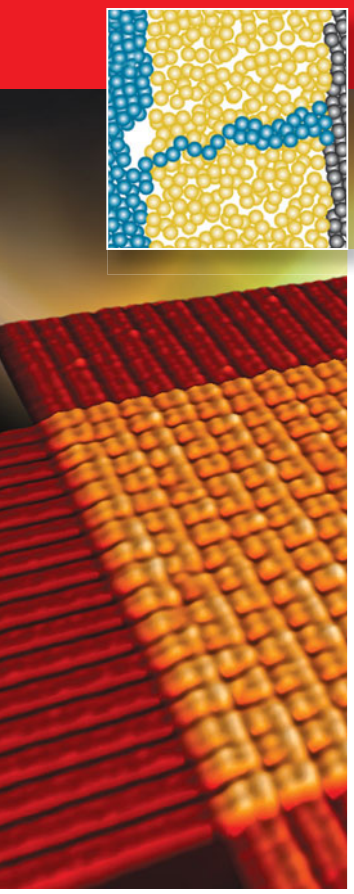


Electrochemical metallization cells—blending nanoionics into nanoelectronics?

Wei Lu, Doo Seok Jeong, Michael Kozicki, and Rainer Waser

A range of material systems exist in which nanoscale ionic transport and redox reactions provide the essential mechanisms for memristive switching. One class relies on mobile cations, which are easily created by electrochemical oxidation of the corresponding electrode metal, transported in the insulating layer, and reduced at the inert counterelectrode. These devices are termed electrochemical metallization (ECM) memories, also called conductive bridge random access memories. The memristive characteristics of the ECM cells provide opportunities for circuit design and computational concepts that go beyond those in traditional complementary metal oxide semiconductor (CMOS) technology. Passive memory arrays open up paths toward ultradense and 3D stackable memory and logic gate arrays. Furthermore, the multivalued conductance characteristics allow for potential exploitation of the cells as synapses in neuromorphic circuits in future energy efficient high-performance computer architectures. Despite exciting results obtained in recent years, many challenges have to be met before these physical effects can be turned into competitive industrial technology. Here, we briefly review the basic working principle, the different possible and potential material combinations, and the fundamental electrochemical processes in ECM cells and their implications for device operations. The prospects of ECM-based resistive random access memory as an emerging memory technology are also reviewed in terms of switching speed and scalability.

Introduction

The semiconductor industry has been persistently seeking an ideal non-volatile memory (NVM) that can simultaneously possess attributes such as high density, high speed, low power consumption, and low cost.[1] Charge-based flash memory represents the state-of-the-art NVM technology at present and is widely adopted in applications from embedded systems to portable electronics and mass storage because of its large capacity and inexpensive manufacturing.[1–3] However, circumventing the problems associated with flash memory, such as limited endurance, slow write speed, and complicated data management schemes, has become more challenging as storage density increases. Moreover, density scaling through continued complementary metal oxide semiconductor (CMOS) scaling also faces several fundamental and technological challenges that will likely reach a limit below 20 nm. As an emerging memory technology, resistive random access memory (RRAM), which is based on a two-terminal device structure that stores data as a change in its resistance, has become a promising candidate due to its simple structure, fast programming, high stacking density, and facile fabrication.

The first true resistance switching devices were originally reported in the 1960s and involved oxides, including SiO_2, sandwiched between a variety of metals in a metal/insulator/metal configuration. Most of the early work focused on unipolar switching in oxides. Systems exhibiting bipolar switching began to appear in the literature in the 1970s. In particular, resistive switching (RS) attributed to the formation and dissolution of an Ag filament in Ag-doped As_2S_3 was reported in 1976 by Hirose et al.[4]

We distinguish among three major types of RS behaviors depending on the switching mechanism.[5,6] One class is based

Wei Lu, University of Michigan, USA; wluee@umich.edu
Doo Seok Jeong, Korea Institute of Science and Technology, Seoul, South Korea; dsjeong@kist.re.kr
Michael Kozicki, Arizona State University, USA; michael.kozicki@asu.edu
Rainer Waser, Forschungszentrum Jülich, Germany; r.waser@fz-juelich.de
DOI: 10.1557/mrs.2012.5

© 2012 Materials Research Society
https://doi.org/10.1557/mrs.2012.5 Published online by Cambridge University Press

on a unipolar thermochemical mechanism or memory effect in which a current-induced temperature increase leads to a fuse/antifuse process. The second class is based on the bipolar valence change mechanism or memory effect that occurs in several transition metal oxides and is triggered by the drift-diffusion of oxygen anions. Based on this class, the term "memristor"[7] in a more general sense has been linked to RS effects,[8] which led to an additional rise in interest in these emerging memory concepts. The third class, based on the bipolar electrochemical metallization mechanism or memory effect (ECM), relies on the electrochemical dissolution and deposition of active electrode metals such as Ag and Cu. This review will focus on these ECM cells, also called conductive bridging RAM (CBRAM) or programmable metallization cells (PMC) in the literature, which have seen tremendous advances recently in materials and device developments toward large-scale applications. For more extensive discussions on ECM cells, the reader is encouraged to consult a recent comprehensive review.[9]

Device structure and material choices

A basic ECM cell is a metal-solid electrolyte-metal system. **Figure 1** sketches the operation principle of an ECM cell in conjunction with a current-voltage switching cycle using a quasi-static triangular voltage signal. The cell consists of an electrode made of an electrochemically active electrode (AE) metal, such as Ag or Cu, an electrochemically inert counter electrode (CE), such as Pt, Ir, or W, and a solid electrolyte layer sandwiched between the AE and CE.[9] In the initial high resistance state (OFF state) of the cell, no electrodeposit of the AE metal is present on the CE (Figure 1a).

A SET (or programming) process occurs if a sufficient positive bias voltage is applied to the AE. The overall SET process involves the following steps, using Ag as an example of the AE and Pt as the CE:[5,6,9]

1. Anodic dissolution of Ag according to the reaction

$$Ag \rightarrow Ag^{+} + e^{-}, \qquad (1)$$

where Ag^{+} represents the monovalent metal cation, the most common oxidation state of Ag, in the solid electrolyte;

2. Drift of the Ag^{+} cations across the solid electrolyte under an applied high electric field;
3. Reduction and electro-crystallization of Ag on the surface of the Pt according to the cathodic deposition reaction

$$Ag^{+} + e^{-} \rightarrow Ag; \qquad (2)$$

4. Growth of the Ag filament.

The electro-crystallization process (Equation 2) leads to the formation of a metal filament growing preferentially toward the AE (Figure 1c). After the metal filament has grown to make an electronic (e.g., galvanic) contact with the AE, the cell has switched to the ON state (Figure 1d). The cell retains the ON state unless a sufficient voltage of opposite polarity is applied and the electrochemical dissolution of the metal filament RESETs the cell (Figure 1e) to its initial OFF state (Figure 1a).

In general, different switching parameters (e.g., a higher switching voltage) are typically required to switch a virgin cell for the first time in a process that is normally termed electroforming or forming. It is conceivable that the initial electroforming process causes structural changes to the electrolyte layer[5,6] and allows subsequent resistance switching to occur at lower voltages. For example, for an SiO_2 electrolyte, it has been suggested that during electroforming, a growing filament in SiO_2 will impose mechanical stress and form nanoscale conduction channels for metal cations, which persist after electrochemical dissolution of the original filament (e.g., Figure 1e).[10] Such a channel could then form the template for subsequent switching events. Details of the forming process, however, may vary significantly depending upon electrolyte materials and cell geometries.

A vast number of combinations of materials fit this basic description of ECM cells, and indeed a wide variety of materials

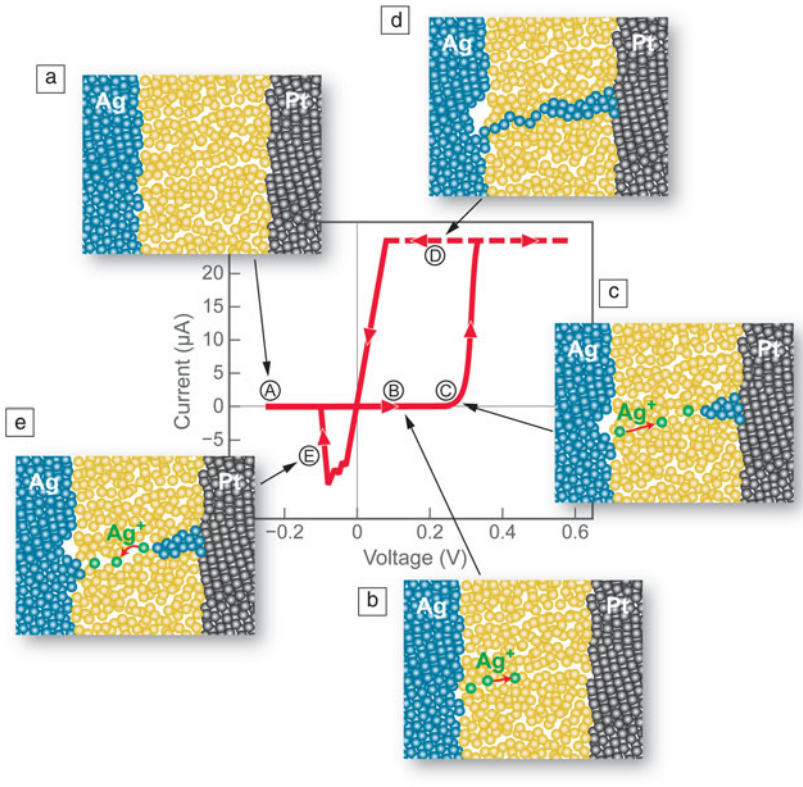


Figure 1. Schematic of the (a–d) SET and (e) RESET operations of an electrochemical metallization (ECM) cell. Reprinted with permission from Reference 9. ©2011, IOP Publishing.

https://doi.org/10.1557/mrs.2012.5 Published online by Cambridge University Press

have been explored for use as ECM materials. **Table I** provides a summary of several material combinations that have been investigated over the past 30 years. Over the past 10 years of research, an extraordinary variety of insulating materials have been utilized as electrolyte layers, even materials not traditionally viewed as good solid electrolytes, such as SiO_2. One reason for this is that the electrolyte can be made very thin, meaning ions from the AE do not have to travel far to form a filament. Thus, even poor ionic conductors can switch quickly, owing to the high electric fields that even modest applied voltages can produce.

Since the source/sink of the ions form a filament, the choice of AE is critical for the operation of ECM cells. Far fewer AE materials have been investigated than CE, as seen in Table I, due to the fact that a narrow window in the electrochemical potential exists for easy redox reactions. The choice of Ag as the AE material in early ECM cells[60,61] was motivated by the use of As_xS_y and related higher chalcogenide electrolytes, which had been extensively studied as prototypical Ag^+ conductors.

Table I. Summary of reported electrochemical metallization cells employing either Ag or Cu as an active electrode (AE) metal and various electrolytes and counter electrode (CE) metals.

Electrolyte	Active electrode (AE) metals	
	Ag	Cu
Ge_xS_y	W[11–19]	W[15]
Ge_xSe_y	W[11,16,20–23] Pt[24] Ni[16,25–27]	W[15]
Ge-Te	TiW[28]	TaN[29]
Ge-Sb-Te	Mo[30]	
As-S	Au[31]	
$Zn_xCd_{1-x}S$	Pt[32,33]	
Cu_2S		Pt[34,35] Ti[36,37]
Ta_2O_5		Pt[38–40] Ru[41]
SiO_2	Co[42]	W[43,44] Pt[10] Ir[45]
WO_3	W[43]	W[43,46]
TiO_2	Pt[47,48]	
ZrO_2	Au[49]	
MSQ	Pt[50,51]	
GdO_x		W[52]
a-Si	Poly-Si[53–55] Cr[56]	
Ge_xSe_y/SiO_x		Pt[57]
Ge_xSe_y/Ta_2O_5		W[58]
Cu_xS/Cu_xO		Pt[59]
Cu_xS/SiO_2		Pt[59]

Electrolyte and CE materials are indicated in each row. For bilayer electrolytes, AE would be placed to the left of the electrolyte (e.g., Cu/A/B/Pt for a cell with a Cu AE metal and A/B bilayer electrolyte). Information compiled by John R. Jameson, Adesto Technologies Corp. Reprinted with permission from Reference 9. ©2011, IOP Publishing.

Nowadays, Cu is also commonly studied as an AE material. Recently, alloys such as CuTe have also been explored as alternative AE materials instead of elemental metals.[52]

The choice of CE material has been driven by the rather straightforward requirements that the CE should be sufficiently inert (i.e., no electrochemical dissolution should occur during RESET operation) and that it be compatible with future large-scale fabrication. The latter requirement is of lesser concern for fundamental research, making Pt a common choice in university laboratories. At the industrial level, W is seen as a natural choice, as standard processes already exist for manufacturing W vias.[12,19,23] For ECM arrays employing some of the materials combinations listed in Table I and utilizing the 1T1R (one transistor for device selection and one RS element) architecture, key performance data are summarized in **Table II**.

Electrochemistry and kinetics of ECM

ECM switching speed can be limited by the kinetics of the redox reactions of the AE material at either the anode or the cathode, or by the kinetics of cation transport through the electrolyte layer. The measure for constrictions in the electrode reaction rate is the overpotential ($\Delta\varphi$), defined as the deviation of the potential from that at equilibrium. What determines the electrode reaction ($M^{z-} + zc- \leftrightarrow M$) is the overpotential $\Delta\varphi_H$ assigned to the Helmholtz double layer at the electrolyte/electrode interface, as shown in **Figure 2**. $\Delta\varphi_H$ can be assigned to the initial crystallization process $\Delta\varphi_{crystal}$ and the charge transfer process through the Helmholtz double layer $\Delta\varphi_{charge}$, and thus $\Delta\varphi_H = \Delta\varphi_{crystal} + \Delta\varphi_{charge}$. The initial crystallization can be observed mainly for reversible processes and generally at lower overpotentials (up to roughly 50 mV). Details on the effects of the crystallization overpotential on the ECM cell performance are given in Reference 5.

The free energy of the oxidized state of the redox reaction (i.e., $M^{z+} + ze^-$, where M^{z+} and ze^- are separated by the Helmholtz double layer) is shifted by $ze\Delta\varphi_{charge}$ because the electrochemical potential of the electrons changes by the same amount, $\Delta\varphi_{charge}$. However, the free energy of the reduced state (i.e., M) is not affected by $\Delta\varphi_{charge}$ due to its charge neutrality. Therefore, the formation free energy of the reaction, $M^{z+} + ze^- \leftrightarrow M$, as well as the activation barrier height is given by a function of $\Delta\varphi_{charge}$.

The Faradaic current versus voltage relationship for this redox reaction controlled by charge transfer at steady state conditions is given by the Butler-Volmer equation:

$$i = i_0\left[\exp\left(\frac{(1-\alpha)ze}{k_BT}\Delta\varphi_{charge}\right) - \exp\left(\frac{-\alpha ze}{k_BT}\Delta\varphi_{charge}\right)\right], \quad (3)$$

where i is the Faradaic current density; i_0 is the exchange current density; α is the transfer coefficient; and z_i is the number of exchanged electrons. The first term on the right side of Equation 3 denotes the anodic process (oxidation), $M \rightarrow M^{z+} + ze^-$, and the second term the cathodic process (reduction) $M^{z+} + ze^- \rightarrow M$. The exchange current density defines the current density at equilibrium where the Faradaic current is zero. The Butler-Volmer

https://doi.org/10.1557/mrs.2012.5 Published online by Cambridge University Press

Table II. Summary of key performance data reported to date in electrochemical metallization arrays.

Material Systems	$Cu/Cu_2S/Ti$	$Cu\text{-}Te/GdO_x/W$	$Ag/Ge_xS_y/W$	Ag/Ge_xS_y or Ge_xSe_y
Reference	Kaeriyama et al.[37]	Aratani et al.[52]	Gopalan et al.[19]	Dietrich et al.[63]
Array Size Tested	1 kbit	4 kbit	384 kbit, 1 Mbit	2 Mbit
Technology Node	250 nm	180 nm	180 & 130 nm	90 nm
SET Condition	1.1 V/5–32 μs	3 V/5 ns/110 μA	1.5 V/250 ns/30 μA	≥0.6 V/≤50 ns/10 μA
RESET Condition	1.1 V/5–32 μs	1.7 V/1 ns/125 μA	0.6 V/12 ms/20 μA	≤0.2 V/≤50 ns/20 μA
Endurance	10^3–10^4	10^7	10^5	10^6
Retention (measured)	10^3 s @ 35 mV	100 hours @ 130°C	24 hours @ 110°C	10^5 s @ 70°C
Retention (projected)	3 months	10 years	10 years @ 70°C	10 years

All arrays utilized 1T1R (one transistor for device selection and one resistive switching element) architecture. Compiled with information from Chen[62] with the addition of data recently reported for $Ag/Ge_xS_y/W$ cells.[19]

equation is derived for a single step electron transfer case and does not account for additional effects (e.g., multi-step processes, double layer effects). However, for the description of the ECM cells of monovalent cations (e.g., Ag^+), no other terms are needed in the equation.

Unlike liquid electrolytes containing a high concentration of mobile ions with high mobility, the diffuse double layer may not be present in the solid electrolyte of ECM cells; the solid electrolyte may be much thinner than the electric field screening length corresponding to the diffuse double layer thickness. In this case, cation drift by an internal electric field, rather than diffusion, plays a role in the migration of cations. Note that the diffusion direction is opposite to the drift so that it leads to depolarization. The drift-diffusion theory for ions is well described for bulk materials that are regarded as ideally diluted solutions under a small electric field satisfying a first-order approximation. However, ECM cells may not satisfy this condition. High electric fields due to the very thin electrolyte layer and high concentration of dissolved cations may make the unmodified drift-diffusion theory not suitable for the description of ECM cells. Exponential dependence on the electric field similar to Equation 3 has been observed experimentally.[10,13,25,34,64,65]

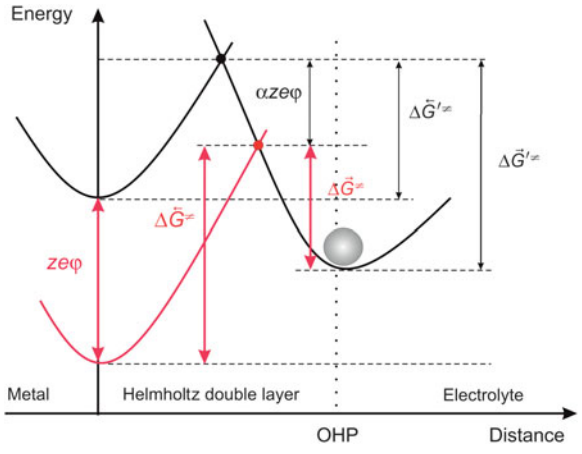


Figure 2. Free energy diagram of a charge transfer process. The black curves represent the initial state, and the red curve results after applying an electric potential to the metal electrode. OHP is the outer Helmholtz plane. $\Delta\bar{G}'^{\neq}$, $\Delta\bar{G}'^{\neq}$, $\Delta\bar{G}^{\neq}$, and $\Delta\bar{G}^{\neq}$ represent the activation free energy for the forward and backward reactions without and with an applied voltage, respectively. Reprinted with permission from Reference 9. ©2011, IOP Publishing.

The kinetics of the filament formation process and corresponding SET switching speed can be limited by the following factors that are of series contributions: (1) the anodic dissolution of the AE; (2) the migration of the metal ions through the electrolyte; (3) the reduction of the ions to metal at the CE (limited by charge transfer, drift-diffusion, or crystallization); and (4) the filament growth. It is estimated that anodic dissolution may be a fast process due to the high electric fields ensuring sufficient decrease of the energy barrier maximum, shown in Figure 2 at the anode interface. Another approach models the anodic dissolution as the rate-limiting step and deduces an exponential rate dependence.[66] Concerning process (2), metal ion migration can be the rate-determining factor depending on the diffusion coefficient or mobility of the electrolyte used, though the electrolyte is very thin. For instance, filament formation in several insulators of low diffusion coefficients of *extrinsic* cations (e.g., SiO_2, amorphous Si, Ta_2O_5, WO_3) may be limited by process (2). The exponential dependence of the SET speed on voltage, as shown in **Figure 3**, might reflect the exponential field-dependence of the underlying ionic migration, as several studies have suggested, despite the fact that an evaluation of the corresponding equation typically leads to unrealistically large ion hopping distances. The metal deposition process at the CE (i.e., process 3) is likely to be the slowest process, as it is also related to space expansion due to new phase formation, which strongly suppresses the electro-crystallization rate and, in turn, limits the growth rate of the filament. According to a study on Ag-GeSe systems by means of potentiodynamic methods,[67] the reduction of Ag ions at the CE determines the

https://doi.org/10.1557/mrs.2012.5 Published online by Cambridge University Press

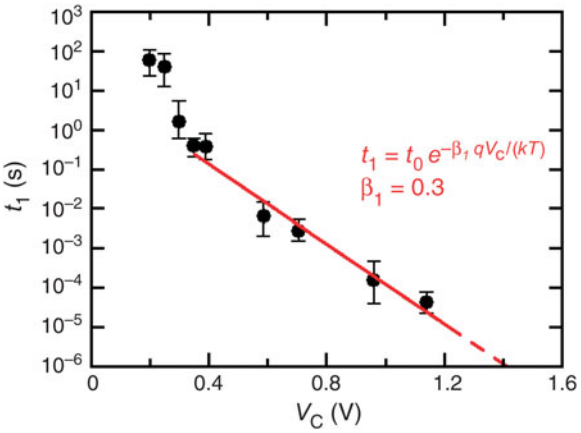


Figure 3. Exponential dependence of the SET speed, t_1, on the SET voltage, V_C. Device structure was Ag/Ge_xS_y/W. Reprinted with permission from Reference 13. ©2009, IEEE.

overall reaction rate and, therefore, the switching speed during the SET process in this system.

It follows from the discussion that all three stages, processes (1–3), during filament formation can be the rate-limiting process under any given experimental conditions, so that it is difficult to offer a universal answer. Therefore, one should carefully go through each process for the system under investigation and compare the rate of each process in order to answer the question about the rate-limiting process.

Implications for device performance

RS in ECM cells can take place in the ns (nanosecond) range with only a few volts of applied voltage.[50,52] This implies that the dissolution and electro-crystallization occur at the ns scale. An example is a Pt/MSQ/Ag/Pt ECM cell with 100 nm line width reliably programmed with 10 ns, ±3.5 V write/erase voltage pulses, as seen in **Figure 4**. Moreover, the programming current of ECM cells has been shown to be as low as a few nA.[45] In contrast, the requirement of the retention performance of ECM cells as an NVM dictates that the device maintains its state for about 10 years with minimal read disturbance. Because the read voltage, limited by the thermal voltage (~26 mV at room temperature), cannot be much smaller than approximately one-tenth of the programming voltage, the rate-limiting processes in ECM cells must still be sufficiently nonlinear in order to meet the change of ~16 orders of magnitude in time scales from ns during programming to 10 years retention for reading. This "voltage-time dilemma"[5] in practice places a restriction on screening out potential NVM devices. Fortunately, it has been shown that the rates of metal dissolution and crystallization have exponential dependence on applied voltages, making it possible to overcome the voltage-time dilemma in ECM cells. In this case, it is desirable to choose materials with high energy barriers for charge transfer, which favors long retention. The loss in speed can be compensated by using high programming electric fields to take advantage of the exponential speed up.

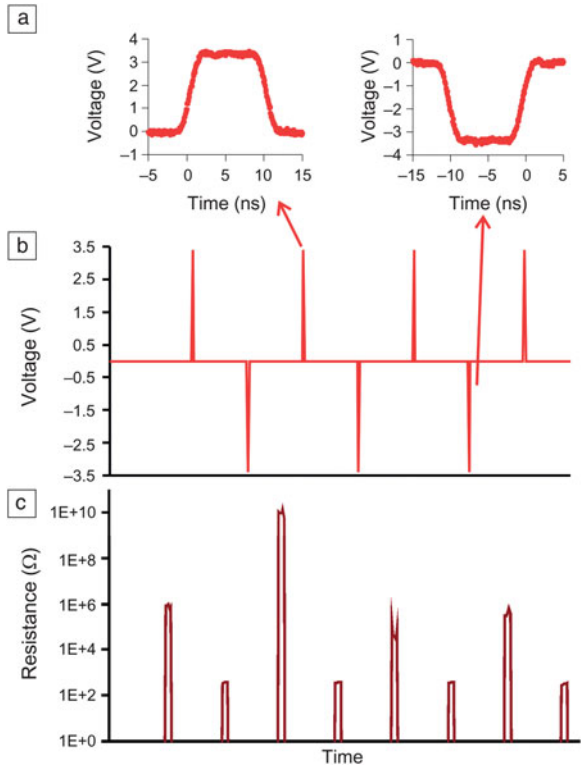


Figure 4. Pulse measurements on a Pt/MSQ/Ag/Pt electrochemical metallization (ECM) cell. (a) Shape of applied voltage pulses, (b) series of pulses, and (c) the measured resistance. Reprinted with permission from Reference 13. ©2009, IEEE.

However, since the decisive rate-limiting processes in individual ECM systems may be different, careful analysis needs to be performed for different systems to achieve device optimizations in light of overcoming the voltage-time dilemma.

The retention of the ON (SET) state is a critical issue, whereas the OFF (RESET) state of ECM cells is quite stable over long periods of time, even at elevated temperatures.[12,23,37] An interesting observation (e.g., References 12 and 13 for Ag/Ge_xS_y/W cells) is that the retention of the ON state improves as the value of R_{ON} decreases. An explanation pointed out by several authors[13,14] is that lower values of R_{ON} correspond to thicker, or perhaps multiple, metal filaments, which would presumably be slower to "erode" away. This implies that the retention of ECM cells depends on the SET/RESET algorithm that is used, as R_{ON} depends strongly on factors such as the current compliance used for SET.

Scaling potential, integration, and prospects

ECM cells are considered to be highly scalable devices, owing to the fact that current in the ON state is presumably carried by a very narrow filament. The key piece of evidence normally cited for scalability is that the resistance of the ON-state does not depend, or depends only weakly, on the area of the device. The excellent scalability of ECM cells has been demonstrated

https://doi.org/10.1557/mrs.2012.5 Published online by Cambridge University Press

directly in a number of studies (e.g., 30 nm in diameter for Cu_2S-based cells[36] and 20 nm for Ge_xSe_y-based[23] and GdO_x-based[52] cells). Furthermore, in particular $Pt/Ag_2S/Ag/Pt$ crossbar cells, it has been shown that the ON resistance can be controlled down to quantum conductance levels ($2e^2/h$) and changed in discrete steps. Observations of the quantum conductance steps suggest that ECM cells could be scaled down to the true atomic level.[65,66]

ECM cell arrays can be active, utilizing a transistor to access each memory cell, or passive, in which each cell has a diode-like device in series with the storage element to provide cell-to-cell isolation. Active arrays, in which each cell contains one transistor for device selection and one RS element (1T1R), have been demonstrated by various groups.[19,21] The area of an individual cell in the 1T1R approach is governed in this case not by the storage element but by the select transistor area, which is typically $8F^2$ to $6F^2$ (where F is the minimum feature size) if DRAM select transistors are used. A second drawback to the 1T1R approach is that the transistors have to be fabricated in the Si substrate, making it difficult to achieve multilayer stacking of the cells for higher storage densities.

A diode-isolated passive array, in which each cell contains one RS element and one diode (1D1R) as the selection device, is a more compact alternative than the 1T1R approach.[55,68–72] The diode plays a role in preventing so-called sneak currents through unselected cells in the network. Zener or breakdown diodes rather than conventional PN diodes are compatible with ECM cells, which require bipolar applied signals for SET/RESET.[72] The main advantage of the 1D1R approach is that it may achieve a design rule of $4F^2$, much smaller than the 1T1R scheme, and enables multi-stacking memory arrays. However, the fabrication of compatible integrated diodes has been a significant challenge.

A different approach to overcome the sneak path problem and to operate large passive crossbar arrays is based on complementary resistive switches (CRS),[73] as briefly mentioned in the introductory article. In CRS, each memory cell is composed of two anti-serial (complementary) interconnected ECM cells but with no additional selection devices.[73] It is worthwhile noting that since no additional transistors or diodes are required, the CRS approach can be highly scalable. The internal operation of ECM-based CRS cells has been confirmed experimentally,[74] and an interactive demonstration is available online.[75]

With the many merits discussed previously, ECM memory is a leading candidate for next generation NVM, potentially replacing existing charge-based Flash and DRAM memories as a universal memory technology. Looking into the future, further advances will be required to address the temperature tolerance issue of some electrolyte materials and demonstrate the retention robustness when the filament is further scaled to the (several) nm regime.

Further outlook for applications of ECM cells

Beyond applications in high-density memory for data storage, electrochemical metallization (ECM) devices have attracted interest in a broad range of applications such as non-volatile standard random access memory (SRAM),[76] reconfigurable logic, and neuromorphic systems. A non-volatile SRAM is expected to effectively reduce standby power consumption presently observed in conventional SRAM cells by storing the state information in a pair of resistive switching cells, such as ECM cells.[76] ECM cells can also be used as switchable interconnects in reconfigurable large-scale-integration circuits, such as field programmable gate arrays.[37,39,77]

The structure and performance of the ECM cells bear many resemblances with those of a synapse—the interconnection between neurons in biological creatures, in the sense that they are both "two-terminal" devices whose resistance can be modified by stimuli applied across them.[78] Several recent studies have attempted to build brain-inspired computing systems by using a crossbar network of ECM cells acting as synapses.[79,80] Compared to conventional CMOS-based logic circuits, the bio-inspired computing approaches offer much better scaling potential and energy efficiency when dealing with complex tasks and, along with memory, can be a main driver for continued material and device development of ECM cells.

Acknowledgments

W.L. would like to thank Dr. Yuchao Yang for his help and the National Science Foundation CAREER award (ECCS-0954621) for partial financial support. D.S.J. would like to acknowledge a KIST research grant (grant no. 2E22123). The authors appreciate the careful consistency check and symbol check by Stefan Tappertzhofen, RWTH Aachen University.

References

1. *International Technology Roadmap for Semiconductors (ITRS), 2010 Edition*; www.itrs.net/Links/2010ITRS/Home2010.htm.
2. A. Chung, J. Deen, J.S. Lee, M. Meyyappan, *Nanotechnology* **21**, 412001 (2010).
3. G.W. Burr, B.N. Kurdi, J.C. Scott, C.H. Lam, K. Gopalakrishnan, R.S. Shenoy, *IBM J. Res. Dev.* **52**, 449 (2008).
4. Y. Hirose, H. Hirose, *J. Appl. Phys.* **47**, 2767 (1976).
5. R. Waser, R. Dittmann, G. Staikov, K. Szot, *Adv. Mater.* **21**, 2632 (2009).
6. R. Waser, M. Aono, *Nat. Mater.* **6**, 833 (2007).
7. L.O. Chua, *IEEE Trans. Circuit Theory* **18**, 507 (1971).
8. D.B. Strukov, G.S. Snider, D.R. Stewart, R.S. Williams, *Nature* **453**, 80 (2008).
9. I. Valov, R. Waser, J.R. Jameson, M.N. Kozicki, *Nanotechnology* **22**, 254003 (2011).
10. C. Schindler, G. Staikov, R. Waser, *Appl. Phys. Lett.* **94**, 072109 (2009).
11. R. Bruchhaus, M. Honal, R. Symanczyk, M. Kund, *J. Electrochem. Soc.* **156**, H729 (2009).
12. R. Symanczyk, R. Bruchhaus, R. Dittrich, M. Kund, *IEEE Electron Device Lett.* **30**, 876 (2009).
13. U. Russo, D. Kamalanathan, D. Ielmini, A.L. Lacaita, M.N. Kozicki, *IEEE Trans. Electron Devices* **56**, 1040 (2009).
14. D. Kamalanathan, U. Russo, D. Ielmini, M.N. Kozicki, *IEEE Electron Device Lett.* **30**, 553 (2009).
15. M.N. Kozicki, M. Balakrishnan, C. Gopalan, C. Ratnakumar, M. Mitkova, *2005 Proc. Non-Volatile Memory Tech. Symp.* 83 (2005).
16. M.N. Kozicki, C. Gopalan, M. Balakrishnan, M. Park, M. Mitkova, *2004 Proc. Non-Volatile Memory Tech. Symp.* 10 (2004).
17. M. Balakrishnan, M.N. Kozicki, C. Gopalan, M. Mitkova, *Device Research Conf. Digest* 47 (2005).
18. D. Kamalanathan, S. Baliga, S.C.P. Thermadam, M. Kozicki, *Proc. Non-Volatile Memory Tech. Symp.* 90 (2007).
19. C. Gopalan, Y. Ma, T. Gallo, J. Wang, E. Runnion, J. Saenz, F. Koushan, P. Blanchard, S. Hollmer, *Solid-State Electron.* **58**, 54 (2011).
20. M.N. Kozicki, M. Mitkova, *J. Non-Cryst. Solids* **352**, 567 (2006).
21. N.E. Gilbert, M.N. Kozicki, *IEEE J. Solid-State Circuits* **42**, 1383 (2007).

https://doi.org/10.1557/mrs.2012.5 Published online by Cambridge University Press

22. R. Symanczyk, M. Balakrishnan, C. Gopalan, T. Happ, M.N. Kozicki, M. Kund, T. Mikolajick, M. Mitkova, M. Park, C.-U. Pinnow, J. Robertson, K.-D. Ufert, *Proc. Non-Volatile Memory Tech. Symp.* 17 (2003).
23. M. Kund, G. Beitel, C.U. Pinnow, T. Rohr, J. Schumann, R. Symanczyk, K.D. Ufert, G. Muller, *IEDM Tech. Dig. 2005*, 773 (2005).
24. C. Schindler, M. Meier, R. Waser, M.N. Kozicki, *Proc. Non-Volatile Memory Tech. Symp.* 81 (2007).
25. M.N. Kozicki, M. Park, M. Mitkova, *IEEE Trans. Nanotechnol.* **4**, 331 (2005).
26. M.N. Kozicki, M. Mitkova, M. Park, M. Balakrishnan, C. Gopalan, *Superlattices Microstruct.* **34**, 459 (2003).
27. M. Mitkova, M.N. Kozicki, *J. Non-Cryst. Solids* **299**, 1023 (2002).
28. C.J. Kim, S.G. Yoon, K.J. Choi, S.O. Ryu, S.M. Yoon, N.Y. Lee, B.G. Yu, *J. Vac. Sci. Technol., B* **24**, 721 (2006).
29. S.-J. Choi, J.-H. Lee, H.-J. Bae, W.-Y. Yang, T.-W. Kim, K.-H. Kim, *IEEE Electron Device Lett.* **30**, 120 (2009).
30. R. Pandian, B.J. Kooi, G. Palasantzas, J.T.M. De Hosson, A. Pauza, *Appl. Phys. Lett.* **91**, 152103 (2007).
31. I. Stratan, D. Tsiulyanu, I. Eisele, *J. Optoelectron. Adv. Mater.* **8**, 2117 (2006).
32. P. van der Sluis, *Appl. Phys. Lett.* **82**, 4089 (2003).
33. Z. Wang, P.B. Griffin, J. McVittie, S. Wong, P.C. McIntyre, Y. Nishi, *IEEE Electron Device Lett.* **28**, 14 (2007).
34. N. Banno, T. Sakamoto, T. Hasegawa, K. Terabe, M. Aono, *Jpn. J. Appl. Phys.* **45**, 3666 (2006).
35. S.-W. Kim, Y. Nishi, *Proc. Non-Volatile Memory Tech. Symp.* 75 (2007).
36. T. Sakamoto, N. Banno, N. Iguchi, H. Kawaura, H. Sunamura, S. Fujieda, K. Terabe, T. Hasegawa, M. Aono, *Symp. VLSI Tech. Dig. Tech.* 38 (2007).
37. S. Kaeriyama, T. Sakamoto, H. Sunamura, M. Mizuno, H. Kawaura, T. Hasegawa, K. Terabe, T. Nakayama, M. Aono, *IEEE J. Solid-State Circuits* **40**, 168 (2005).
38. T. Sakamoto, N. Banno, N. Iguchi, H. Kawaura, H. Sunamura, S. Fujieda, K. Terabe, T. Hasegawa, M. Aono, *Symp. VLSI Tech. Dig. Tech.* 38 (2007).
39. T. Sakamoto, K. Lister, N. Banno, T. Hasegawa, K. Terabe, M. Aono, *Appl. Phys. Lett.* **91**, 092110 (2007).
40. N. Banno, T. Sakamoto, S. Fujieda, M. Aono, *Fourth Annu. Int. Reliab. Symp.* 707 (2008).
41. Y. Tsuji, T. Sakamoto, N. Banno, H. Hada, M. Aono, *Appl. Phys. Lett.* **96**, 023504 (2010).
42. S. Manhart, *J. Phys. D* **6**, 82 (1973).
43. C. Schindler, S.C.P. Thermadam, R. Waser, M.N. Kozicki, *IEEE Trans. Electron Devices* **54**, 2762 (2007).
44. M. Balakrishnan, S.C.P. Thermadam, M. Mitkova, M.N. Kozicki, *2006 Proc. Non-Volatile Memory Tech. Symp.* 104 (2006).
45. C. Schindler, M. Weides, M.N. Kozicki, R. Waser, *Appl. Phys. Lett.* **92**, 122910 (2008).
46. M.N. Kozicki, C. Gopalan, M. Balakrishnan, M. Mitkova, *IEEE Trans. Nanotechnol.* **5**, 535 (2006).
47. K. Abe, M.P. Tendulkar, J.R. Jameson, P.B. Griffin, K. Nomura, S. Fujita, Y. Nishi, *Proc. Int. Conf. IC Design Tech.* 203 (2008).
48. K. Tsunoda, Y. Fukuzumi, J.R. Jameson, Z. Wang, P.B. Griffin, Y. Nishi, *Appl. Phys. Lett.* **90**, 113501 (2007).
49. Y.T. Li, S.B. Long, M.H. Zhang, Q. Liu, L.B. Shao, S. Zhang, Y. Wang, Q.Y. Zuo, S. Liu, M. Liu, *IEEE Electron Device Lett.* **31**, 117 (2010).
50. M. Meier, C. Schindler, S. Gilles, R. Rosezin, A. Rudiger, C. Kugeler, R. Waser, *IEEE Electron Device Lett.* **30**, 8 (2009).
51. C. Kuegeler, C. Nauenheim, M. Meier, A. Ruediger, R. Waser, *Proc. Non-Volatile Memory Tech. Symp.* 59 (2008).
52. K. Aratani, K. Ohba, T. Mizuguchi, S. Yasuda, T. Shiimoto, T. Tsushima, T. Sone, K. Endo, A. Kouchiyama, S. Sasaki, A. Maesaka, N. Yamada, H. Narisawa, *IEDM Tech. Dig. 2007* 783 (2007).
53. S.H. Jo, K.H. Kim, W. Lu, *Nano Lett.* **9**, 870 (2009).
54. S.H. Jo, W. Lu, *Nano Lett.* **8**, 392 (2008).
55. K.H. Kim, S.H. Jo, S. Gaba, W. Lu, *Appl. Phys. Lett.* **96**, 053106 (2010).
56. A.J. Snell, P.G. Lecomber, J. Hajto, M.J. Rose, A.E. Owen, I.S. Osborne, *J. Non-Cryst. Solids* **137**, 1257 (1991).
57. R. Soni, M. Meier, A. Ruediger, B. Hollaender, C. Kuegeler, R. Waser, *Microelectron. Eng.* **86**, 1054 (2009).
58. S.Z. Rahaman, S. Maikap, *Proc. IEEE Int. Memory Workshop* 70 (2010).
59. J. Yi, S.W. Kim, Y. Nishi, Y.T. Hwang, S.W. Chung, S.J. Hong, S.W. Park, *Proc. Non-Volatile Memory Technology Symp.* 32 (2008).
60. W.C. West, K. Sieradzki, B. Kardynal, M.N. Kozicki, *J. Electrochem. Soc.* **145**, 2971 (1998).
61. M.N. Kozicki, W.C. West, U.S. Patent No. 5,761,115 (1998).
62. A. Chen, *2008 Proc. Non-Volatile Memory Tech. Symp.* 27 (2008).
63. S. Dietrich, M. Angerbauer, M. Ivanov, D. Gogl, H. Hoenigschmid, M. Kund, C. Liaw, M. Markert, R. Symanczyk, L. Altimime, S. Bournat, G. Mueller, *IEEE J. Solid-State Circuits* **42**, 839 (2007).
64. S.H. Jo, K.H. Kim, W. Lu, *Nano Lett.* **9**, 496 (2009).
65. K. Terabe, T. Hasegawa, T. Nakayama, M. Aono, *Nature* **433**, 47 (2005).
66. J.R. Jameson, N. Gilbert, F. Koushan, J. Saenz, J. Wang, S. Hollmer, M.N. Kozicki, *Appl. Phys. Lett.* **99**, 063506 (2011).
67. C. Schindler, I. Valov, R. Waser, *Phys. Chem. Chem. Phys.* **11**, 5974 (2009).
68. M.J. Lee, S. Seo, D.C. Kim, S.E. Ahn, D.H. Seo, I.K. Yoo, I.G. Baek, D.S. Kim, I.S. Byun, S.H. Kim, I.R. Hwang, J.S. Kim, S.H. Jeon, B.H. Park, *Adv. Mater* **19**, 73 (2007).
69. S.E. Ahn, B.S. Kang, K.H. Kim, M.J. Lee, C.B. Lee, G. Stefanovich, C.J. Kim, Y. Park, *IEEE Electron Device Lett.* **30**, 550 (2009).
70. B. Cho, T.-W. Kim, S. Song, Y. Ji, M. Jo, H. Hwang, G.-Y. Jung, T. Lee, *Adv. Mater.* **22**, 1228 (2010).
71. W.Y. Park, G.H. Kim, J.Y. Seok, K.M. Kim, S.J. Song, M.H. Lee, C.S. Hwang, *Nanotechnology*, **21** (2010).
72. S. Puthentheradam, D. Schroder, M. Kozicki, *Appl. Phys. A* **102**, 817 (2011).
73. E. Linn, R. Rosezin, C. Kugeler, R. Waser, *Nat. Mater.* **9**, 403 (2010).
74. R. Rosezin, E. Linn, L. Nielen, C. Kuegeler, R. Bruchhaus, R. Waser, *IEEE Electron Device Lett.* **32**, 191 (2011).
75. www.emrl.de/pu_crs.htm#crs-model.
76. W. Wang, A. Gibby, Z. Wang, T.W. Chen, S. Fujita, P. Griffin, Y. Nishi, S. Wong, *IEDM Tech. Dig. 2006* 539 (2006).
77. D.B. Strukov, K.K. Likharev, *Nanotechnology* **16**, 888 (2005).
78. B. Swaroop, W.C. West, G. Martinez, M.N. Kozicki, L.A. Akers, *Proc. Int. Symp. Circuits and Systems* **3**, 33 (1998).
79. S.H. Jo, T. Chang, I. Ebong, B.B. Bhadviya, P. Mazumder, W. Lu, *Nano Lett.* **10**, 1297 (2010).
80. T. Ohno, T. Hasegawa, T. Tsuruoka, K. Terabe, J.K. Gimzewski, M. Aono, *Nat. Mater.* **10**, 591 (2011). □

ACNS 2012
American Conference on Neutron Scattering
June 24-28, 2012 | Georgetown University Hotel and Conference Center
Washington, D.C., USA

CALL FOR PAPERS

SAVE THE DATE
Join us for the sixth American Conference on Neutron Scattering (ACNS 2012). Held at historic Georgetown University in Washington, D.C., the conference will provide essential information on the breadth and depth of current neutron-related research worldwide. This year's conference will feature a combination of invited and contributed talks, posters sessions, tutorials and an industrial exhibit. The last day of the conference features a tour of the NIST Center for Neutron Research. Mark your calendars today and plan to attend ACNS 2012!

SCIENTIFIC PROGRAM
The four-day conference will feature oral and poster presentations covering:

- Plenary and Prize sessions (Invited Speakers ONLY)
- Sources, Instrumentation and Software
- Soft Condensed Matter
- Hard Condensed Matter
- Biology
- Chemistry
- Energy and Engineering Applications
- Neutron Physics

For the most up-to-date information on ACNS 2012, visit **www.mrs.org/acns-2012**

https://doi.org/10.1557/mrs.2012.5 Published online by Cambridge University Press